Research Square

Preprints are preliminary reports that have not undergone peer review.
They should not be considered conclusive, used to inform clinical practice,
or referenced by the media as validated information.

The great divergence of viral hepatitis in China, 2005–2020: vaccine-driven decline, diagnosis-driven rise, and the hepatitis E exception in a five-type surveillance panel

Fei Wang
First Affiliated Hospital of Xi'an Jiaotong University
Yuxin Liu
First Affiliated Hospital of Xi'an Jiaotong University
Yuanyuan Duan
Xian Center for Disease Control and Prevention
Yajuan He
First Affiliated Hospital of Xi'an Jiaotong University
Mi Ke
First Affiliated Hospital of Xi'an Jiaotong University
Tianyan Chen
First Affiliated Hospital of Xi'an Jiaotong University
Zhen Tian
tianzhen@xjtufh.edu.cn

First Affiliated Hospital of Xi'an Jiaotong University

Research Article

Keywords: viral hepatitis, hepatitis E, hepatitis A, surveillance, joinpoint regression, distributed lag non-linear models, climate attribution, China

Posted Date: November 6th, 2026

DOI: https://doi.org/10.21203/rs.3.rs-11300443/v1

License: This work is licensed under a Creative Commons Attribution 4.0 International License.
Read Full License

Additional Declarations: No competing interests reported.

Abstract

Background

China's viral hepatitis landscape has been reshaped by vaccination, expanded diagnostics, and improved laboratory typing, yet the five serotypes have almost always been studied in isolation. Whether the rising reported incidence of hepatitis E—the only enteric type still increasing—reflects transmission, ascertainment, demography, or climate remains unresolved. We compared all five types on the same panel with the same methods.

Methods

We assembled a 31-province, 192-month (2005–2020), age-stratified panel of nationally reported cases and deaths (20 763 781 cases; 12 742 deaths). Joinpoint regression quantified trends; the Edwards test characterised seasonality; Kitagawa decomposition (dual endpoints 2005→2019 and 2005→2020) separated rate from age-structure effects; and identical two-stage distributed lag non-linear models with warming attribution were fitted for hepatitis A and E. Hepatitis E mechanistic estimates are cited from a companion study.

Results

Three trajectories emerged. Hepatitis A fell 10·3% per year (− 20·4% after the 2008 immunization-programme introduction; −96% at ages 5–14); hepatitis B was flat in aggregate (− 0·5% per year) while collapsing 13·9% per year at ages 0–19 and rising 4·1% per year at ages ≥ 60. Hepatitis C rose 10·0% per year before plateauing after 2012; unspecified hepatitis fell 11·9% per year, benchmarking improving ascertainment. Hepatitis E alone rose (+ 3·6% per year), overtaking hepatitis A from 2012; its rise preceded the steepest typing gains and was four-fifths a rate effect. The two enteric types diverged on geography (west versus east), season (summer versus early spring), age (childhood versus old age), and temperature response (negative versus positive). Warming attribution was − 969 cases for hepatitis A versus + 2 300 for hepatitis E. Hepatitis E case fatality (1·09 per 1 000) was threefold that of hepatitis A, with 57% of deaths at ages ≥ 60.

Conclusions

Hepatitis E is neither an ascertainment artefact nor a uniform climate response but the residual frontier of China's hepatitis transition: a foodborne infection of an ageing population, amplified by warmth and unreached by existing interventions. Priorities include routine hepatitis E testing in older adults with acute hepatitis, vaccine evaluation for high-risk and elderly groups, and inclusion of this burden in climate-adaptation planning.

Background

China's viral hepatitis landscape has been reshaped over the past two decades by three intervention lines operating simultaneously. Hepatitis A vaccine entered the national Expanded Programme on Immunization (EPI) in 2008, adding to long-standing neonatal hepatitis B vaccination [1]; blood-supply screening and expanding access to antiviral testing transformed the ascertainment of hepatitis B and C [2]; and improvements in laboratory typing steadily eroded the pool of reported hepatitis that could not be assigned to a serotype. These three lines—vaccination, diagnostic expansion, and classification improvement—constitute a natural set of internal reference frames against which the trajectory of any single hepatitis type can be benchmarked, provided all types are observed under the same surveillance system.

Yet the epidemiological literature has analysed the five types almost exclusively in isolation. Single-disease studies have documented the vaccine-driven decline of hepatitis A [3, 4], the cohort effects of neonatal hepatitis B vaccination [5], the diagnosis-driven surge of hepatitis C [2], and the genotypic shift of hepatitis E from waterborne genotype 1 to zoonotic, food-borne genotype 4 [6]. The only multi-type analyses are descriptive: a recent four-type study characterised spatiotemporal patterns for 2007–2023 using scan statistics and spatial autocorrelation [7], and a country-level modelling study related hepatitis incidence to broad meteorological and hygiene factors at annual ecological resolution [8]. No study has compared all five types on the same panel with the same methods, and none has moved from pattern description to attribution.

The unresolved question is the status of hepatitis E. It is the only enterically transmitted type whose reported incidence has risen over the study period; provincial climate studies disagree even on the sign of the temperature association [9–11]; and whether its rise is real transmission, expanded testing, demographic ageing, or climate is contested [6, 11]. These hypotheses cannot be adjudicated from hepatitis E data alone: they require the counterfactual behaviour of the other types under the same system—what a vaccine-driven decline, a diagnosis-driven rise, and a classification-driven collapse each look like.

We therefore analysed a 31-province, 192-month, age-stratified surveillance panel of all five viral hepatitis types in China (2005–2020), with three aims: to characterise the divergence of the five types under common trend, seasonality, and spatial frameworks; to benchmark hepatitis E against the internal reference frames of vaccine-driven decline and diagnostic improvement; and to contrast the two enterically transmitted types—hepatitis A and E—under identical climate-attribution methods. A companion nationwide study examines the climatic and demographic drivers of hepatitis E in depth, including a quasi-experimental analysis of the 2019 African swine fever shock and burden projections to 2050 [12]; its hepatitis E estimates are cited here as reference values, and all comparative, hepatitis A, and cross-type analyses are new to this study. In distinction to previous descriptive multi-type work, we use the collapsing pool of unspecified hepatitis as an internal benchmark for diagnostic improvement and the vaccine-preventable types as benchmarks for intervention-driven decline, to test whether the rise

of hepatitis E is an artefact of ascertainment or a uniform climate response—or a genuine exception requiring its own explanation.

Methods

Study design and data sources

We conducted a nationwide ecological time-series study comparing all five serotypes of viral hepatitis under a single surveillance system. Monthly counts of reported viral hepatitis cases and deaths by province and single-year age (0, 1, 2, …, ≥85 years) from January 2005 to December 2020 were obtained from the Chinese Public Health Science Data Center [13], covering all 31 provincial-level administrative divisions of mainland China. Reported cases are classified in the surveillance system as hepatitis A (HAV), hepatitis B (HBV), hepatitis C (HCV), hepatitis D (HDV), hepatitis E (HEV), and viral hepatitis of unspecified type; both clinically diagnosed and laboratory-confirmed cases are included under national reporting criteria. The summed counts of the five typed categories plus the unspecified category equalled the independently reported total for every province–month (internal consistency 100%), and national annual totals were reconciled against officially published figures (difference <2% in the validation year, 2013). Over the 192 study months, the panel comprised 20 763 781 reported cases and 12 742 deaths. For analysis, single-year ages were aggregated into three bands (0–19, 20–59, and ≥60 years); records with unknown age (≈0% of cases) were excluded from age-band analyses.

Provincial annual population denominators, overall and by the three age bands, were interpolated from national censuses and annual statistical yearbooks (2005–2020) [14]. Monthly mean temperature and precipitation by province were derived from the 0·25° × 0·25° CN05.1 gridded observational dataset (the dataset is provided by Arid Land Ecology and Resources Science Data Center, https://data.dcxjegi.cn) [15]; monthly relative humidity was obtained from NASA POWER [16]. Annual provincial covariates (gross domestic product per capita, urbanisation rate, hospital beds per 1 000 population) were compiled from national statistical yearbooks [14].

The study uses anonymised, aggregated surveillance counts and publicly available statistics; institutional review board approval and informed consent were not required.

Temporal trend analysis (joinpoint regression)

For each hepatitis type, we computed national annual incidence rates and fitted log-linear joinpoint regression models [18] by exhaustive grid search over candidate joinpoint years, with the number of joinpoints (0–3) selected by the Bayesian information criterion. We report the annual percent change (APC) for each segment and the average annual percent change (AAPC) for the full period, weighted by segment width. Because 2020 reporting was disrupted by the COVID-19 response (national notifiable disease reports fell by approximately 41% in 2020 [17]), the primary window was 2005–2019, with 2005–

2020 fitted as a sensitivity analysis. To decompose the aggregate HBV trend by vaccination-cohort exposure, identical models were fitted separately to the three age bands.

Seasonality (Edwards test)

National monthly case counts for 2005–2019 were aggregated by calendar month, adjusted for month length, and tested for cyclical variation with the Edwards test [19]. We report the peak month (angular mean) and the seasonal amplitude R (the magnitude of the first harmonic as a percentage of the annual mean).

Provincial patterns

Provincial mean annual incidence rates were computed for two periods (2005–2009 and 2015–2019) using annual population denominators, and the period ratio (fold change) was calculated for each province and type.

Temperature–incidence relations (two-stage distributed lag non-linear models)

To benchmark the climate sensitivity of the two enterically transmitted types against each other, we fitted two-stage distributed lag non-linear models (DLNM) [20, 21] for hepatitis A, applying the same specification previously validated for hepatitis E in a companion nationwide study [12]. In stage one, province- and age-band-specific negative-binomial generalised linear models regressed monthly case counts on a cross-basis of monthly mean temperature (natural cubic spline with knots at the tertiles of the pooled temperature distribution) over lags 0–2 months (spline lag space), adjusting for precipitation (spline), relative humidity, a long-term time trend (spline with knots at 2010 and 2015), calendar month (indicator), socio-economic covariates (log GDP per capita, urbanisation rate, hospital beds per 1 000 population), and a policy indicator for the July 2008 inclusion of hepatitis A vaccine in the national Expanded Programme on Immunization (EPI). The population offset was log(population/12). The negative-binomial dispersion parameter was selected by profile likelihood over a grid; when the primary specification failed to converge or yielded a non-positive-definite covariance matrix, a prespecified fallback specification (linear precipitation, year fixed effects) was used. In stage two, province-specific coefficient vectors were pooled by multivariate random-effects meta-analysis (DerSimonian–Laird estimator); between-province heterogeneity was summarised with Cochran's Q and I^2. Cumulative exposure–response curves over lags 0–2 months are reported relative to each band's median temperature reference. Sensitivity analyses excluded the year 2020.

Warming attribution

For each age band, temperature-attributable cases were estimated following the Gasparrini counterfactual framework [22]: the observed temperature series was compared with a detrended series obtained by removing the province-specific Theil–Sen trend (robust to endpoint anomalies, preserving the seasonal cycle), and attributable cases were computed from the pooled exposure–response curve relative to the minimum-risk temperature (estimated within the 5th–95th percentile range). Warming-attributable cases were defined as the difference between attributable cases under observed and detrended temperature.

Trend decomposition (Kitagawa)

Changes in the national crude rate were decomposed into age-structure (composition) and age-specific-rate effects using the Kitagawa (Oaxaca–Blinder two-component) method [23]. Following the dual-endpoint reporting specification established in the companion study, both 2005→2019 and 2005→2020 decompositions are reported, because COVID-19 artefacts can dominate single-endpoint contrasts.

Sensitivity and validation analyses

Four analyses probed the robustness of the comparison layer. First, vaccine-attributed decline of hepatitis A was examined by vaccine-type grouping: provinces using the two-dose inactivated vaccine under the EPI (Beijing, Tianjin, Shanghai, Jiangsu) were compared with the 27 provinces using the one-dose live attenuated vaccine [3]; Zhejiang switched to inactivated vaccine only in 2022 and was retained in the live-vaccine group for the study window. Second, vaccine supply sufficiency during the EPI period was assessed from national batch-release volumes of hepatitis A vaccines compiled from public National Institutes for Food and Drug Control announcements [24] (figures verified against primary per-batch records in the NIFDC batch-release database, which published quantities through February 2021; Additional file 1). Full joinpoint segments, seasonality statistics, decomposition and attribution detail, and vaccine-group sensitivity results are provided in Additional file 2 (Tables S2–S7 and Figure S1).. Third, potential diagnostic overlap between adult hepatitis A and E in eastern provinces—where reported hepatitis A shows an anomalous spring peak—was examined by comparing the age composition of the March excess cases with the age spectrum of hepatitis E and with the paediatric seasonal template. Fourth, the companion study's findings on hepatitis E (temperature relation, trend decomposition, the 2019 African swine fever quasi-experiment, and projections) were used as cited reference values only and were not re-estimated here, to avoid duplicate presentation [12].

Analyses used Python 3·12·14 (statsmodels 0·15·0, pandas 3·0·2, numpy 2·4·4; DLNM and multivariate meta-analysis implemented following the dlnm/mvmeta frameworks [20, 21]). Two-sided $p<0·05$ was considered significant.

Results

The great divergence: five types, three trajectories

Between January 2005 and December 2020, 20 763 781 viral hepatitis cases and 12 742 deaths were reported across the 31 provinces. The five typed categories diverged into three distinct trajectories over the study period (Figure 1; Table 1).

Vaccine-preventable decline. Reported hepatitis A incidence fell from 5·70 to 1·38 per 100 000 between 2005 and 2019 (AAPC −10·3% per year), with the steepest decline immediately after the 2008 EPI inclusion of hepatitis A vaccine (APC −20·4% during 2007–2012). The decline was nearly identical in provinces using inactivated vaccine and those using live attenuated vaccine (0–19 years: −91·0% versus −93·3% between 2008 and 2019), and national batch-release volumes of the single-dose live vaccine alone (21·1 million doses in 2019 and 20·2 million in 2020, NIFDC per-batch records) exceeded the annual birth cohort by 44% and 68%, respectively, indicating that supply was not a constraint. Declines were concentrated in vaccine-cohort ages: cases at ages 5–9 and 10–14 years both fell by 96%. Hepatitis B showed an apparently stable national trend (AAPC −0·5%), but this aggregate masked a cohort cross-section: incidence at ages 0–19 fell from 47·9 to 6·0 per 100 000 (AAPC −13·9%), while incidence at ages ≥60 *rose* from 50·9 to 88·3 per 100 000 (AAPC +4·1%)—a flat total concealing simultaneous collapse in vaccinated cohorts and growth in unvaccinated, ageing ones (Figure 5).

Diagnosis-driven rise. Hepatitis C rose from 3·9 to 16·0 per 100 000 between 2005 and 2019 (AAPC +10·0%), but with a clear saturation pattern: APC decelerated from +30·7% (2005–2007) to +0·9% after 2012, consistent with expansion and subsequent saturation of testing rather than unbounded transmission growth.

The classification anchor. Unspecified hepatitis collapsed from 5·3 to 0·9 per 100 000 (AAPC −11·9%; −81·8% in absolute counts), accelerating after 2014 (APC −17·3%). This monotonic contraction of the untyped pool provides an internal benchmark for diagnostic improvement against which the trajectories of the typed categories can be read.

The hepatitis E exception. Against these three reference frames, hepatitis E was the only enterically transmitted type whose incidence rose (1·2 to 2·0 per 100 000; AAPC +3·6%), overtaking hepatitis A in annual case counts from 2012. Critically, the rise was not monotonic: incidence increased steeply during 2005–2011 (APC +14·4% during 2008–2011) and then entered a high plateau (APC −0·3%, 2011–2019). The persistence of this plateau while the unspecified pool continued to fall at −17% per year argues against ascertainment as the sole explanation for the rise. Hepatitis E also carried the heaviest mortality burden among the five types: crude case fatality was 1·09 per 1 000—3·1-fold that of hepatitis A (0·35 per 1 000)—and 57·2% of hepatitis E deaths occurred at ages ≥60, where case fatality reached 1·98 per 1 000, four-fold that at ages 0–19.

Provincially, the divergence was not an artefact of national averaging (Figure 2). During 2015–2019, hepatitis A burden concentrated in the west (highest in Xinjiang, 9·7, and Qinghai, 5·9 per 100 000), whereas hepatitis E concentrated in the middle–lower Yangtze and the southeast coast (Hubei 4·7,

Hainan 4·5, Jiangsu 3·4). Between 2005–2009 and 2015–2019, hepatitis A incidence fell in nearly all provinces while hepatitis E rose in most—opposite-signed fold changes across the 31-province panel.

Seasonality was formally significant for all five types (Edwards test, all p<0·001; Figure 2), but hepatitis E stood out with both the strongest seasonal amplitude (R=14·0% of the annual mean) and the earliest peak (March). Hepatitis A peaked in early July (amplitude 5·2%), and the remaining types showed modest spring peaks (amplitude 3·3–5·1%).

The hepatitis A–E mirror: same panel, same methods, opposite signatures

The two enterically transmitted types—epidemiologically the closest pair in the panel—diverged most sharply once examined with identical methods, forming a mirror image across four dimensions (Figures 3, 4; Table 2).

Season and place. Hepatitis E peaked sharply in March nationally (monthly index 150·5; east 153·5), whereas hepatitis A peaked in late summer—most distinctly in western provinces (August–October indices 114–116), the same provinces carrying the highest hepatitis A burden. The spatial–seasonal crossover is exact: the enteric hepatitis of the western summer is hepatitis A; the enteric hepatitis of the eastern spring is hepatitis E (Figure 2).

Age. The age gradients pointed in opposite directions. Hepatitis E incidence at ages ≥60 was 33-fold that at ages 0–19 (3·99 versus 0·12 per 100 000 per year), and within the ≥60 band the oldest subgroup grew fastest: cases at ages ≥80 rose 3·6-fold between 2005 and 2019 (278 to 994), their share of the ≥60 burden increasing from 6·8% to 10·0%. Hepatitis A showed the reverse gradient (≥60 to 0–19 rate ratio 0·7), with incidence highest in childhood. Within the same viral family, one disease belongs to children and the other to the elderly.

Temperature response. Under identical two-stage DLNM specifications, the pooled temperature–incidence curves crossed at the reference temperature in the 20–59-year band: hepatitis A responded negatively to warmth (cumulative RR at 29·2°C 0·84 [95% CI 0·64–1·11]; RR at −12·9°C 1·26 [0·76–2·11]) while hepatitis E responded positively (RR at 29·2°C 1·13 [0·84–1·52]; at −12·9°C 0·70 [0·43–1·16]) (Figure 3). At ages 0–19, hepatitis A was significantly cold-associated (RR 3·40 [1·02–11·32] at the cold extreme), although this association attenuated and lost significance when 2020 was excluded (RR 2·29 [0·68–7·69]); we therefore report it as direction-consistent but limited in strength. At ages ≥60, the two curves converged: both were monotonically positive and nearly identical in slope (hepatitis A RR 1·58 [1·06–2·36] at 29·2°C; hepatitis E 1·66 [1·21–2·27]; between-province heterogeneity I^2=0% for hepatitis E in all bands and 0–23% for hepatitis A).

Attribution. The mirrored exposure–response curves translate into mirrored climate accounts. Over the 16 years of observed warming, the counterfactual attribution assigns approximately −970 cases to

hepatitis A (net protection: −638 at ages 0–19 and −808 at ages 20–59, partly offset by +477 at ages ≥60) against approximately +2 300 cases for hepatitis E (companion-study estimate) (Table 2). Warming is simultaneously eroding the cold-season niche of hepatitis A and amplifying hepatitis E: climate change is reshaping the *relative* burden of the two enteric hepatitis types in opposite directions. Trend decomposition sharpens the same contrast from the demographic side (Table 2): the hepatitis A decline is a pure rate phenomenon—age structure contributed 0·6% of the 2005→2019 crude-rate change, and the dual endpoints (2019; 2020) yield identical conclusions—whereas for hepatitis E the companion study showed a genuine rate increase (79%) compounded by population ageing (21%), with the 2020 endpoint alone producing a misleading 96% structure share. Hepatitis A's endpoint robustness and hepatitis E's endpoint sensitivity, estimated under one framework, jointly demonstrate why dual-endpoint reporting is necessary.

Diagnostic overlap. One caution qualifies the mirror. The anomalous spring (March) peak of hepatitis A in eastern provinces is concentrated in adults: 83% of the March excess occurred at ages 20–59 and 12% at ages ≥60—an age composition closer to that of hepatitis E (65·7% at 20–59; 33·0% at ≥60) than to paediatric hepatitis A, which retains the classic summer peak in the same provinces (August index 139·6 versus March 116·6 at ages 0–19). Part of the reported adult "hepatitis A" spring signal in the east is therefore likely to reflect delayed differential diagnosis or misclassification with hepatitis E; a genuine adult spring transmission route (for example, shellfish) cannot be excluded. This overlap also offers a parsimonious explanation for the convergence of the two temperature curves at ages ≥60.

Positioning the exception. Taken together, the three reference frames and the mirror comparison establish that the hepatitis E rise is neither an ascertainment artefact (the untyped pool kept collapsing through the plateau years), nor a demographic artefact (rate effects dominate), nor a generic climate response shared by all enteric hepatitis (hepatitis A moves in the opposite direction under the same climate field). A companion nationwide study attributes the residual mechanism to a food-borne, zoonotic (genotype 4) regime in an ageing population, including a measurable suppressive fingerprint of the 2019 African swine fever pork-price shock [12]; the present analysis adds the comparative anatomy: hepatitis E is also the most strongly seasonal of the five types, and its climate sensitivity is systematically opposite to that of its closest epidemiological relative.

Positioning the exception: synthesis

The five-type panel offers a compact summary of China's hepatitis transition. Between 2005 and 2019, the vaccine-preventable types contracted (hepatitis A −10·3% per year; hepatitis B stable in aggregate but collapsing in vaccinated cohorts), the diagnosis-expanding type rose and saturated (hepatitis C +10·0% per year, plateauing after 2012), and the untyped residual drained away (−11·9% per year)—three trajectories that jointly trace the reach of China's vaccination and diagnostic systems. Hepatitis E escapes all three frames. Its rise (+3·6% per year) began before the steepest gains in typing coverage, persisted as a plateau through years when the untyped pool was still falling at −17% per year, is

dominated by genuine rate increases rather than compositional change, and—uniquely among the enteric types—its climate sensitivity runs with, not against, the warming trend.

Read against the companion study's mechanistic findings [12], the comparative evidence converges on a regime interpretation: China's hepatitis E is no longer the waterborne, outbreak-prone disease of the historical record (the 1986–1988 Xinjiang outbreak being the canonical case [25, 26]), but a sporadic, food-borne infection of an ageing population, amplified modestly and uniformly by warmth, concentrated among older adults (case fatality at ages ≥60: 1·98 per 1 000), and sensitive to shocks in the pork supply chain. The mirror comparison with hepatitis A shows what this regime is not: not climate-driven in the way a waterborne enteric infection is (hepatitis A), not vaccine-reachable under the current immunization programme, and not explained by the expansion of testing that accounts for hepatitis C. For surveillance and control, the five-type panel thus reframes hepatitis E from an anomaly in a declining family into the family's residual frontier: the type against which existing intervention lines have so far been silent.

Discussion

In a single 31-province, 192-month, age-stratified panel observed under one surveillance system, the five types of viral hepatitis in China followed three distinct trajectories between 2005 and 2019: vaccine-preventable types contracted (hepatitis A − 10·3% per year, with the steepest decline, − 20·4% per year, immediately following the 2008 EPI introduction; hepatitis B stable in aggregate but falling − 13·9% per year among 0–19-year-olds), the diagnosis-expanding type rose and saturated (hepatitis C + 10·0% per year, plateauing after 2012), and the untyped residual drained away (− 11·9% per year). Hepatitis E alone rose as a genuine exception (+ 3·6% per year, plateauing after 2011), overtaking hepatitis A in annual case numbers from 2012—a crossover independently corroborated in provincial surveillance analyses [11]. A recent four-type analysis described overlapping spatiotemporal patterns for 2007–2023 [7]; the present study moves from pattern description to attribution. Three features carry the argument beyond description: the collapsing unspecified category serves as an internal benchmark that absorbs the ascertainment explanation for hepatitis E; identical two-stage climate-attribution methods applied to the two enteric types yield opposite-signed warming contributions (− 969 versus + 2 300 attributable cases); and dual-endpoint decomposition (2005→2019 primary, 2005→2020 sensitivity) separates durable demographic signals from COVID-era reporting artefacts.

The three trajectories map onto three intervention lines, and each sharpens the interpretation of the others. The hepatitis A decline, concentrated in school-age cohorts (− 96% among 5–14-year-olds) and steepest in the western provinces with a summer peak, is the signature of a vaccine interrupting childhood transmission of a waterborne infection—externally consistent with programme evaluations of the Expanded Hepatitis A Programme [4] and with national modelling linking hepatitis A incidence negatively to temperature [8]. The hepatitis B aggregate, flat at − 0·5% per year, conceals a cohort transition: vaccinated birth cohorts are replacing unvaccinated ones (− 87% in rates among 0–19-year-olds) while reported incidence among adults ≥ 60 years rose 4·1% per year, most plausibly reflecting expanded testing and care-seeking in an ageing chronically infected pool. This divergence carries a

general methodological lesson for surveillance interpretation: aggregate trend statistics for long-incubation, chronically prevalent infections can remain benign precisely while the underlying epidemiology is being transformed, and age-stratified or cohort analyses are the minimum requirement for reading such series. The hepatitis C plateau after 2012 and the accelerated collapse of unspecified hepatitis after 2014 (− 17·3% per year) jointly date the maturation of China's laboratory typing capacity. Against this internally dated ascertainment calendar, hepatitis E's rise began too early (steepest 2008–2011), persisted too long, and—per the Kitagawa decomposition—is four-fifths a rate effect rather than compositional change: ascertainment cannot be its primary engine.

The mirror comparison localises what hepatitis E is. The two enteric types share transmission routes yet diverge in every comparative dimension: geography (west versus east), season (summer versus early-spring peak), demography (childhood versus old age), and climate response (negative versus positive temperature associations among working-age adults). The early-spring (March) hepatitis E peak—strongest seasonal signature of any type (Edwards R = 14·0%)—sits awkwardly with its positive temperature association: incidence is amplified by warmth in monthly models, yet peaks in the cold season. This temporal mismatch points to a behavioural-foodborne driver operating on a calendar (winter pork consumption concentrated around the Spring Festival) that is independent of, and stronger than, the meteorological cycle [6]; the companion study's quasi-experimental analysis of the 2019 African swine fever shock—which cut China's swine inventory by roughly 40% [27]—provides direct evidence that pork-supply disruption transmits measurably into hepatitis E incidence [12]. Hepatitis A shows the mirror image of this logic: its 0–19-year-old cold-temperature association (RR 3·40 at low temperatures), attenuating to non-significance when 2020 is excluded, is consistent with residual winter transmission settings rather than a stable climate driver.

Two clinical observations follow from the age dimension. First, the temperature–incidence curves of the two enteric types converge at ages ≥ 60 years (RR at 29·2°C: hepatitis A 1·58 [1·06–2·36]; hepatitis E 1·66 [1·21–2·27]), suggesting that in older adults both infections behave as opportunistic illnesses of a susceptible, comorbidity-burdened host rather than as transmission-dynamic diseases. Second, the residual early-spring excess of hepatitis A in eastern provinces is concentrated in working-age and older adults (83% and 12% of the March excess, respectively)—the age profile of hepatitis E, not of childhood hepatitis A—raising the possibility of residual misclassification or genuine shared foodborne exposure. Both observations converge on one practice implication: in older adults presenting with acute hepatitis in China, hepatitis E now carries a case fatality (1·98 per 1 000 at ages ≥ 60; overall 1·09 per 1 000, threefold that of hepatitis A) and an incidence exceeding hepatitis A since 2012, and should be included in the routine differential with serological testing rather than treated as a diagnosis of exclusion [11].

The policy gap is the absence of any population-level intervention line for hepatitis E comparable to those that bent the other curves. The world's only licensed hepatitis E vaccine (Hecolin, Xiamen Innovax) is not included in China's immunization programme and reaches negligible volumes (82 502 doses released in 2019 and 40 975 doses in 2020, with a single batch released in the first four months of 2021; NIFDC batch-release records) [24], despite cost-effectiveness analyses supporting vaccination of high-

risk and older populations [28, 29]. Our results sharpen the target profile in three ways: the burden is concentrated in, and shifting towards, adults ≥ 60 years (cases + 142% over the period; the ≥ 80 share of elderly cases rose from 6·8% to 10·0%); the deaths are overwhelmingly elderly (57% at ages ≥ 60); and the climate attribution indicates that warming will add to, not subtract from, this burden (+ 2 300 attributable cases over 2005–2020, with the elderly share growing)—in direct contrast to hepatitis A, where warming is net protective. For climate adaptation planning, the enteric hepatitis portfolio in China is thus not simply shrinking: its centre of gravity is shifting from a vaccine-controlled childhood infection to an unvaccinated, foodborne infection of old age.

This study has limitations. First, the design is ecological: province-month aggregates cannot establish individual-level causation, and the temperature estimates are associations conditioned on the DLNM specification. Second, surveillance data reflect reporting as well as incidence; although the unspecified-type benchmark and the saturation pattern of hepatitis C bound the ascertainment explanation for hepatitis E, type-specific testing uptake is unobserved, and the eastern hepatitis A spring excess suggests residual misclassification cannot be excluded. Third, the 2020 COVID-19 shock depressed reporting across all types; we mitigated this with dual endpoints and no-2020 sensitivity analyses, but the 2005→2020 Kitagawa decomposition for hepatitis E illustrates that COVID-era endpoints can invert composition conclusions and should not be interpreted demographically. Fourth, genotype is not captured in surveillance; the genotype-1-to-genotype-4 transition is inferred from the literature [6] rather than observed in the panel. Fifth, the regulator publishes batch-release quantities only through February 2021; vaccine-supply corroboration therefore rests on per-batch volumes for 2019–2020 and on batch counts thereafter. Finally, hepatitis E mechanistic results are cited from a companion study whose publication status is pending; the comparative conclusions here stand on analyses internal to this panel, but the mechanistic interpretation should be read jointly with that work.

Conclusions

Under common observation and common methods, China's five hepatitis types trace three trajectories—vaccine-driven decline, diagnosis-driven rise, and classification-driven collapse—against which hepatitis E stands as a genuine exception: rising on rate, not composition; warming-amplified, not warming-eroded; concentrated in the elderly, not in children. Hepatitis E is the residual frontier of China's hepatitis transition. The priorities that follow are concrete: include hepatitis E in the routine serological differential of acute hepatitis in older adults; evaluate deployment of the licensed hepatitis E vaccine for high-risk and elderly populations; and incorporate the rising elderly enteric-hepatitis burden into climate-adaptation planning.

Abbreviations

AAPC: average annual percent change; APC: annual percent change; ASF: African swine fever; CI: confidence interval; DLNM: distributed lag non-linear model; EPI: Expanded Programme on Immunization; GDP: gross domestic product; HAV: hepatitis A virus; HBV: hepatitis B virus; HCV:

hepatitis C virus; HDV: hepatitis D virus; HEV: hepatitis E virus; NIFDC: National Institutes for Food and Drug Control; RR: relative risk

Declarations

Ethics approval and consent to participate

Not applicable. The study uses anonymised, aggregated surveillance counts and publicly available statistics; institutional review board approval and informed consent were not required.

Consent for publication

Not applicable. The manuscript contains no data from any individual person.

Availability of data and materials

The surveillance data that support the findings of this study are available from the Chinese Public Health Science Data Center (https://www.phsciencedata.cn), but restrictions apply: the data were used under a data-use agreement for the current study and so are not publicly available. Data are however available from the authors upon reasonable request and with permission of the Chinese Public Health Science Data Center. Meteorological data are publicly available from the CN05.1 gridded dataset (https://data.dcxjegi.cn) [15] and NASA POWER (https://power.larc.nasa.gov/) [16]; population and socio-economic denominators are from the China Statistical Yearbook [14]. The analysis code is available from the corresponding author on reasonable request. Vaccine batch-release records were extracted from the weekly public announcements of the National Institutes for Food and Drug Control (https://bio.nifdc.org.cn/pqf/search.do?formAction=pqfGs) and are provided in full as Additional file 1 (Supplementary Table S1).

Competing interests

The authors declare that they have no competing interests.

Funding

This work was supported by the Natural Science Basic Research Program Youth Project of the Shaanxi Provincial Science and Technology Department (No. 2023-JC-QN-0830). The funding body played no role in the design of the study, the collection, analysis, and interpretation of data, or in writing the manuscript.

Authors' contributions

FW, YL, and ZT conceived and designed the study. FW, MK, and YL acquired the surveillance, meteorological, and census data and curated the analysis datasets. FW performed the statistical analysis and drafted the manuscript, with methodological support from YH and YL. YD and YL contributed to data validation, quality control, and the literature review. YD contributed virological and surveillance expertise and assisted with acquisition and interpretation of the surveillance data. YH and YL accessed and verified the underlying data and contributed to drafting and revision of the manuscript. TC and ZT supervised the study, contributed to the interpretation of the results, and critically revised the manuscript for important intellectual content. ZT acquired the funding and is the guarantor of the work. FW and YL contributed equally to this work and share first authorship. All authors had full access to all the data in the study, read and approved the final manuscript, and accept responsibility for the decision to submit for publication.

Acknowledgements

We thank the Data-center of China Public Health Science and the Arid Land Ecology and Resources Science Data Center for data access. The CN05.1 dataset is provided by the Arid Land Ecology and Resources Science Data Center (https://data.dcxjegi.cn).

References

1. Cui F, Shen L, Li L, et al. Prevention of chronic hepatitis B after 3 decades of escalating vaccination policy, China. Emerg Infect Dis. 2017;23(5):765–72.
2. Mei X, Lu H. Prevalence, diagnosis, and treatment of hepatitis C in mainland China. Glob Health Med. 2021;3(5):270–5. 10.35772/ghm.2021.01080.
3. Sun X, Wang F, Zheng H, Miao N, Yuan Q, Cui F, Yin Z, Zhang G, Levine H. The impact of expanded program on immunization with live attenuated and inactivated Hepatitis A vaccines in China, 2004–2016. Vaccine. 2018;36(10):1279–84. 10.1016/j.vaccine.2018.01.043.
4. Wu Y, Wang P, Huang Y, Chen J, Chang Y, Li J, Wang Y, Hao Y, Zhang W, Du Z. Assessing the effectiveness of the expanded hepatitis A vaccination program in China: an interrupted time series design. BMJ Glob Health. 2024;9(2):e013444. 10.1136/bmjgh-2023-013444.
5. Liang X, Bi S, Yang W, et al. Epidemiological serosurvey of hepatitis B in China—declining HBV prevalence due to hepatitis B vaccination. Vaccine. 2009;27:6550–7.
6. Wang J, Coughlan S, Li F, Gonzalez G, Fanning S, Li N, Dong Y, Jiang T. Hepatitis E virus: a foodborne pathogen of concern in China. One Health Adv. 2025;3:13. 10.1186/s44280-025-00080-4.
7. Liu Q, Li YF. Spatial and temporal analysis of viral hepatitis in mainland China from 2007 to 2023: implications for targeted public health interventions. Front Public Health. 2025;13:1660415. 10.3389/fpubh.2025.1660415.

8. Sun N, He F, Sun J, Zhu G. Viral hepatitis in China during 2002–2021: epidemiology and influence factors through a country-level modeling study. BMC Public Health. 2024;24:1820. 10.1186/s12889-024-19318-8.
9. Zhao X, Li M, Haihambo N, Wang X, Wang B, Sun M, Guo M, Han C. Periodic characteristics of hepatitis virus infections from 2013 to 2020 and their association with meteorological factors in Guangdong, China: surveillance study. JMIR Public Health Surveill. 2023;9:e45199. 10.2196/45199.
10. Yang L, Wang J, Peng J, Zhang L, Cheng X. Associations of ambient temperature and heat waves with risks of hepatitis E in Jiangsu, China (2010–2023): a time-stratified case-crossover study. Infect Dis Model. 2026;11(1):268–77. 10.1016/j.idm.2025.10.003.
11. Shi Y, Shen W, Liu W, Zhang X, Shang Q, Cheng X, Bao C. Analysis of the spatial-temporal distribution characteristics of hepatitis E in Jiangsu province from 2005 to 2020. Front Public Health. 2023;11:1225261. 10.3389/fpubh.2023.1225261.
12. Wang F, Ke M, Duan Y, He Y, Liu Y, Chen T, Tian Z. Hepatitis E in China, 2005–2020: a food-borne disease of an ageing population — nationwide temperature sensitivity, demographic decomposition, the 2019 African swine fever fingerprint, and burden projections to 2050. Under review.
13. Chinese Center for Disease Control and Prevention. Chinese Public Health Science Data Center: viral hepatitis notifiable-disease surveillance data by province, month and age group, 2005–2020 [data set]. Beijing: Chinese Center for Disease Control and Prevention; [year]. Available from: https://www.phsciencedata.cn/Share/. Accessed [access date]. Restricted access under data-use agreement [agreement number].
14. National Bureau of Statistics of China. China Statistical Yearbook 2006–2021. Beijing: China Statistics.
15. Wu J, Gao XJ. A gridded daily observation dataset over China region and comparison with the other datasets. Chin J Geophys. 2013;56(4):1102–11.
16. NASA POWER Project. Monthly meteorological parameters. NASA Langley Research Center. https://power.larc.nasa.gov/
17. Chen B, Wang M, Huang X, Xie M, Pan L, Liu H, Liu Z, Zhou P. Changes in incidence of notifiable infectious diseases in China under the prevention and control measures of COVID-19. Front Public Health. 2021;9:728768. 10.3389/fpubh.2021.728768.
18. Kim HJ, Fay MP, Feuer EJ, Midthune DN. Permutation tests for joinpoint regression with applications to cancer rates. Stat Med. 2000;19:335–51.
19. Edwards JH. The recognition and estimation of cyclic trends. Ann Hum Genet. 1961;25:83–6.
20. Gasparrini A, Armstrong B, Kenward MG. Distributed lag non-linear models. Stat Med. 2010;29:2224–34.
21. Gasparrini A, Armstrong B, Kenward MG. Multivariate meta-analysis for non-linear and other multi-parameter associations. Stat Med. 2012;31:3821–39.
22. Gasparrini A, Leone M. Attributable risk from distributed lag models. BMC Med Res Methodol. 2014;14:55.

23. Kitagawa EM. Components of a difference between two rates. J Am Stat Assoc. 1955;50:1168–94.
24. National Institutes for Food and Drug Control. Biological product batch-release announcements. Available from: https://bio.nifdc.org.cn/pqf/search.do?formAction=pqfGs. Accessed 2026-10-08.
25. Zhuang H, Cao XY, Liu CB, Wang GM. Epidemiology of hepatitis E in China. Gastroenterol Jpn. 1991;26(Suppl 3):135–8.
26. Aye TT, Uchida T, Ma XZ, Iida F, Shikata T, Zhuang H, Win KM. Complete nucleotide sequence of a hepatitis E virus isolated from the Xinjiang epidemic (1986–1988) of China. Nucleic Acids Res. 1992;20(13):3512. 10.1093/nar/20.13.3512.
27. USDA Economic Research Service. African swine fever shrinks pork production in China, swells demand for imported pork. Amber Waves. 2020 Feb.
28. Cheng X, Zhao Y, Zhang X, Jin H, Min J. Health economic evaluation of immunization strategies of hepatitis E vaccine for elderly population. Hum Vaccin Immunother. 2017;13(8):1873–8. 10.1080/21645515.2017.1316913.
29. Wang F, Zhou L, Lu Y. Cost-effectiveness analysis of hepatitis E vaccination strategies for swine workers. Transbound Emerg Dis. 2025;2025:9371055. 10.1155/tbed/9371055.

Tables

Table 1. Five types of viral hepatitis in China, 2005–2020

Type	Cases (deaths)	AAPC 2005–2019, % (joinpoints)	Peak month (Edwards R)	≥60 vs 0–19 rate ratio	Top-burden provinces 2015–2019, per 100 000
Hepatitis A	571 552 (200)	−10·3 (2007, 2012, 2014)	6·7 (R=5·2%)	0·7	Xinjiang 9·7; Qinghai 5·9; Liaoning 4·5
Hepatitis B	16 533 417 (9 704)	−0·5 (2007, 2012, 2014)	4·2 (R=3·7%)	3·5	Qinghai 163·6; Xinjiang 152·9; Hainan 139·4
Hepatitis C	2 656 625 (1 897)	+10·0 (2007, 2009, 2012)	4·1 (R=3·3%)	21·9	Xinjiang 42·0; Qinghai 35·8; Inner Mongolia 30·4
Hepatitis E	388 867 (423)	+3·6 (2007, 2008, 2011)	3·0 (R=14·0%)	33·0	Hubei 4·7; Hainan 4·5; Jiangsu 3·4
Unspecified	611 639 (518)	−11·9 (2007, 2008, 2014)	4·7 (R=5·1%)	2·6	Fujian 4·4; Anhui 3·7; Liaoning 2·9

Legend: burden, trend, seasonality, and age structure by type. HDV: 1 681 cases, 0 deaths, reported in text only. AAPC: average annual percent change.

Table 2. The attribution mirror: hepatitis A versus hepatitis E

Component	Hepatitis A	Hepatitis E
Crude-rate change 2005→2019, per 100 000	−4·33	+0·80†
— age-structure effect	−0·03 (0·6%)	+0·17 (21%)†
— age-specific-rate effect	−4·30 (99·4%)	+0·63 (79%)†
Dual-endpoint robustness (2005→2020)	unchanged (−4·65; structure 0·7%)	Δ+0·14; structure share 96% (COVID endpoint artefact)†
Temperature response, 20–59 y (RR at 29·2°C vs reference)	0·84 (0·64–1·11)	1·13 (0·84–1·52)†
Temperature response, ≥60 y (RR at 29·2°C)	1·58 (1·06–2·36)	1·66 (1·21–2·27)†
Warming-attributable cases, 2005–2020 (0–19 / 20–59 / ≥60 / total)	−638 / −808 / +477 / **−969**	−49 / +1 247 / +1 102 / **+2 300**†

Legend: outcomes under identical methods. † Hepatitis E estimates from the companion nationwide study [12], cited as reference values; all hepatitis A estimates are new to this study. RR: relative risk.

Figures

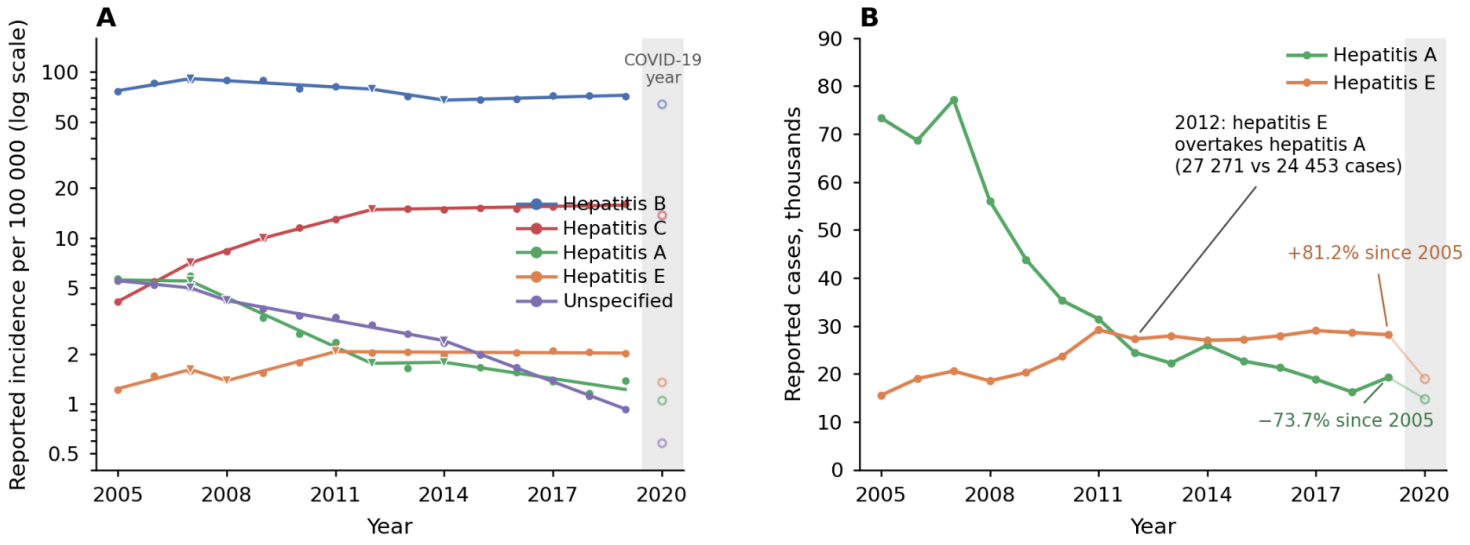


Figure 1

The great divergence of five hepatitis types in China, 2005–2020. (A) National annual reported incidence per 100 000 (log scale); points are observed values, lines are joinpoint piecewise log-linear fits

(2005–2019 model), triangles mark joinpoints. (B) Annual reported cases of hepatitis A and E, showing the 2012 crossover. The 2020 COVID-19 year (grey band, open markers) was excluded from trend fitting.

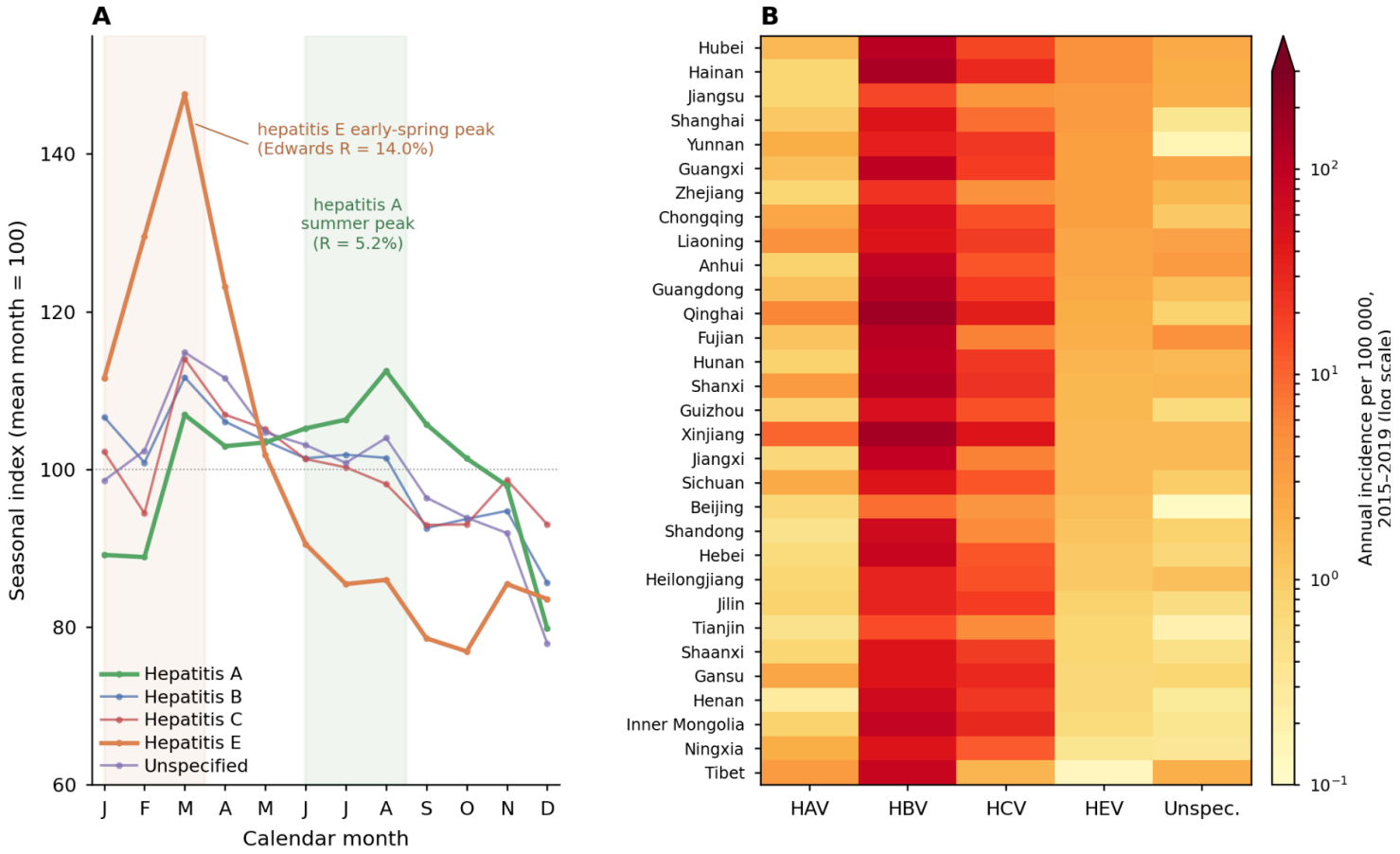


Figure 2

Seasonality and spatial patterns of the five hepatitis types.(A) Day-adjusted monthly seasonal index (mean month = 100), 2005–2019, for the five types; hepatitis E shows the strongest seasonality (Edwards R = 14·0%, peak month March) and hepatitis A a summer peak (R = 5·2%). All five types p < 0·001. (B) Province × type heatmap of average annual reported incidence per 100 000, 2015–2019 (log colour scale), provinces ordered by hepatitis E rate; hepatitis A concentrates in the west, hepatitis E in the east.

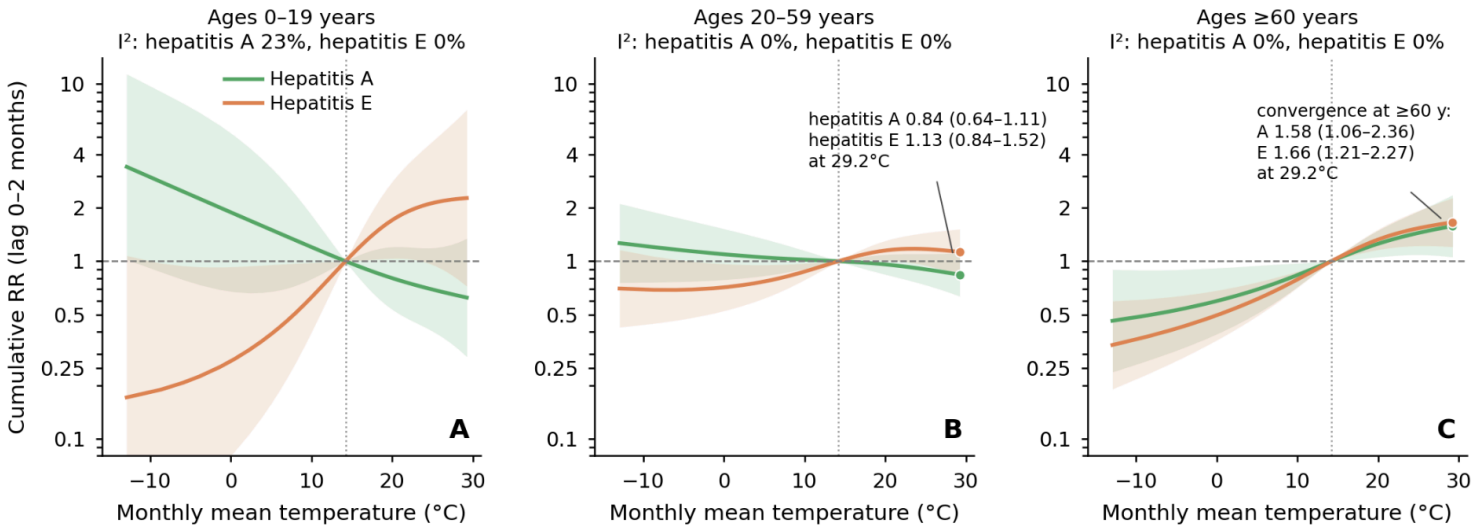


Figure 3

The enteric mirror: pooled temperature–incidence curves by age band. Cumulative relative risk (lag 0–2 months) of monthly mean temperature versus province-specific median (14·2°C), from two-stage distributed lag non-linear models fitted identically for hepatitis A (green) and E (orange), by age band (A: 0–19 y; B: 20–59 y; C: ≥60 y). Shading: 95% CI. At 29·2°C the working-age responses point in opposite directions (A: 0·84 [0·64–1·11]; E: 1·13 [0·84–1·52]); at ages ≥60 the curves converge (A: 1·58 [1·06–2·36]; E: 1·66 [1·21–2·27]).

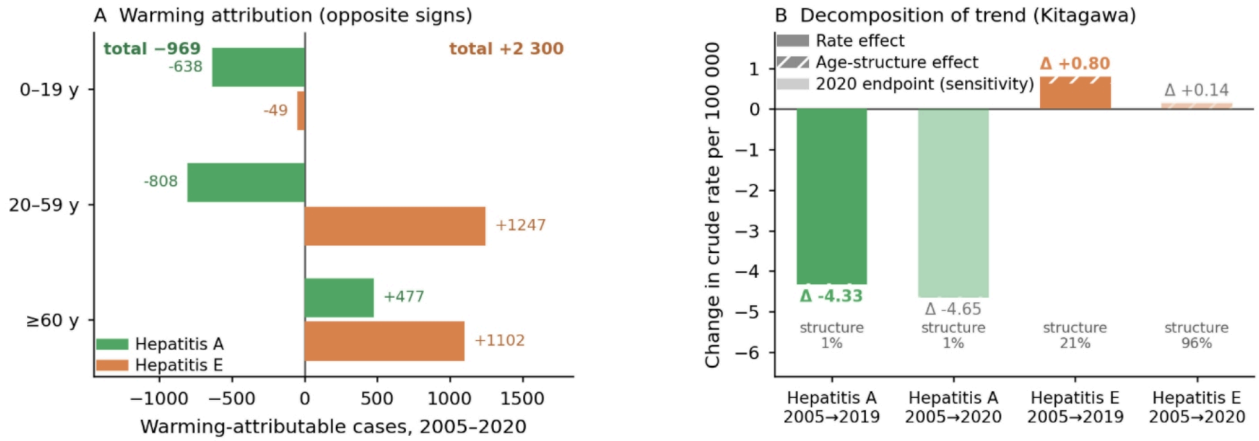


Figure 4

The attribution mirror: warming attribution and trend decomposition. (A) Warming-attributable reported cases, 2005–2020, by age band: net −969 for hepatitis A versus +2 300 for hepatitis E (hepatitis E

estimates from the companion study). (B) Kitagawa decomposition of the change in crude rate per 100 000 from 2005 to 2019 (primary) and 2020 (sensitivity endpoint); the 2020 endpoint artefactually converts the hepatitis E rise into a 96% age-structure effect.

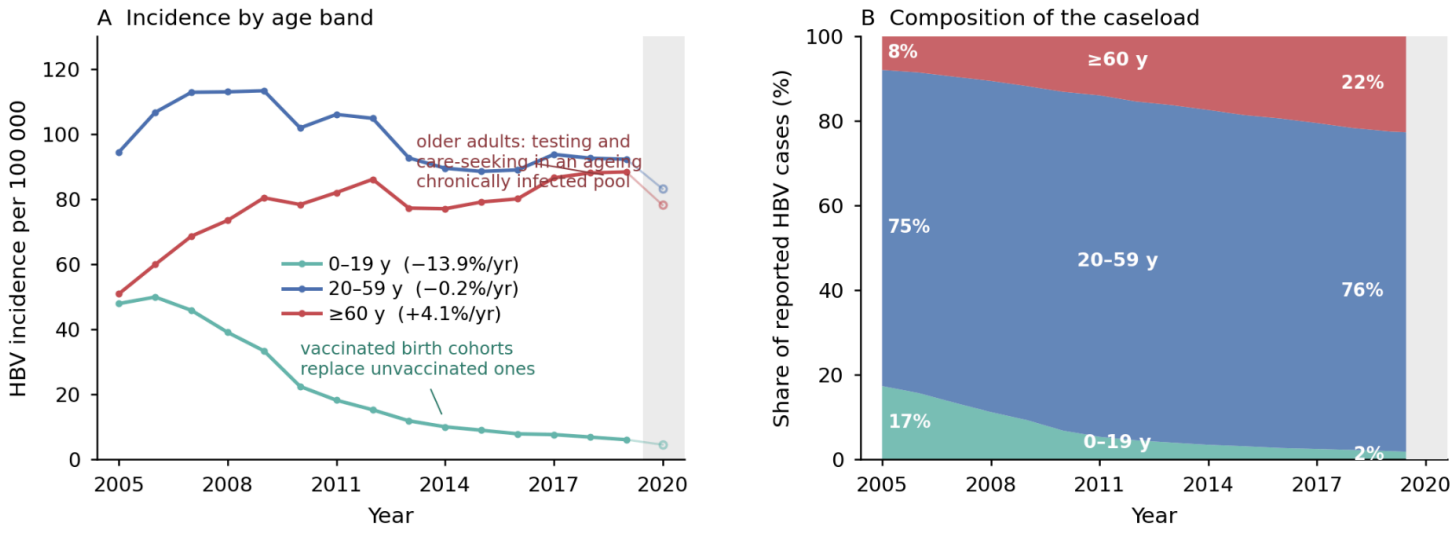


Figure 5

The hepatitis B cohort transition beneath a flat aggregate. (A) HBV reported incidence by age band, 2005–2020: −13·9% per year at ages 0–19, +4·1% per year at ages ≥60, flat overall. (B) Share of reported HBV cases by age band: the 0–19 share collapsed from 17% to 2% while the ≥60 share rose from 8% to 22%.

Supplementary Files

This is a list of supplementary files associated with this preprint. Click to download.

- 04Additionalfile1TableS1.xlsx
- 05Additionalfile2supplementary.docx